VOLUME 120, NUMBER 49
DECEMBER 16, 1998

JOURNAL OF THE AMERICAN CHEMICAL SOCIETY

Photochromism of Spirooxazines in Homogeneous Solution and Phospholipid Liposomes

Rafail F. Khairutdinov,[†] Keturah Giertz,[†] James K. Hurst,*[,†] Elena N. Voloshina,[‡] Nikolai A. Voloshin,[‡] and Vladimir I. Minkin[‡]

Contribution from the Department of Chemistry, Washington State University, Pullman, Washington 99164-4630, and Institute of Physical & Organic Chemistry, Rostov University, 344104 Rostov on Don, Russia

Received July 22, 1998

Abstract: The photochromic behavior of several spirooxazines (SO) containing phenanthrene or phenanthroline moieties in the oxazine part of molecules has been investigated in several solvents and phosphatidylcholine (PC) liposomes. The solvatochromic properties of the merocyanine (MC) forms of these dyes were used to probe their location within the PC membrane. Transient spectroscopic measurements revealed that, when first formed by photoexcitation, the MC forms of phenanthroline-containing spirooxazines were located at relatively nonpolar sites within the membrane, but they subsequently moved to a more polar environment typical of the aqueous−organic interface. The characteristic time for this intersite movement was $\tau \approx 10^{-3}$ s, corresponding to a diffusion coefficient of $D \approx 10^{-11}$ cm^2 s^{-1}. In contrast, these spectral shifts were not observed when PC liposome-bound SO containing the phenanthrene moiety were photoexcited, suggesting that either intersite diffusion was more rapid for these compounds or the initially formed MC (and its spiro precursor) were located in a more polar microenvironment. The rate of thermal ring-closing following UV photoexcitation decreased modestly when either an electron-withdrawing group was present on the MC oxazine ring or an electron-donating group was present on the MC indoline ring. A dramatic increase in the ring-closing rate was observed for an o-phenanthroline-containing SO coordinated to a Ru(bpy)$_2^{2+}$ metal center, an effect attributable to strong donation of electron density from the Ru(II) d-orbitals into the ligand π*-orbitals.

Introduction

Spirooxazines (SO), like other compounds that exhibit photochromic behavior, are potentially applicable as reversible memory photodevices and optical switching elements in molecular electronics.[1−4] Furthermore, spatial or polarity changes accompanying their photoisomerization may be utilized to alter microenvironments within polymers and supramolecular assemblies such as Langmuir−Blodgett films, micelles, and liposomes.[5−8] Spirooxazines have greater photostability than the more widely studied structurally similar spiropyran com-

* Correspondence should be addressed to this author.
[†] Washington State University.
[‡] Rostov University.

(1) *Introduction to Molecular Electronics*; Petty, M. C., Bryce, M. R., Bloor, D., Eds.; Edward Arnold: London, 1995.
(2) Mirkin, C. A.; Ratner, M. A. *Annu. Rev. Phys. Chem.* **1992**, *43*, 719−754.
(3) Bertelson, R. C. In *Photochromism*; Brown, G. H., Ed.; Wiley-Interscience: New York, 1971; pp 733−840.
(4) Chu, N. Y. C. In *Photochromism: Molecules and Systems*; Durr, H., Bouas-Laurent, T. H., Eds.; Elsevier: Amsterdam, 1990; pp 879−882.
(5) Willner, I. *Acc. Chem. Res.* **1997**, *30*, 347−356.
(6) Negishi, N.; Iida, T.; Ishihara, K.; Shinohara, I. *Makromol. Chem., Rapid Commun.* **1981**, *2*, 612−615.
(7) Pieroni, O.; Fissi, A.; Viegi, A.; Fabbri, D.; Ciardelli, F. *J. Am. Chem. Soc.* **1992**, *114*, 2734−2736.
(8) Ishiwari, T.; Kondo, T.; Mitsuishi, M. *Colloid. Polym. Sci.* **1996**, *274*, 1000−1005.

10.1021/ja9825985 CCC: $15.00
Published on Web 12/01/1998

Scheme 1

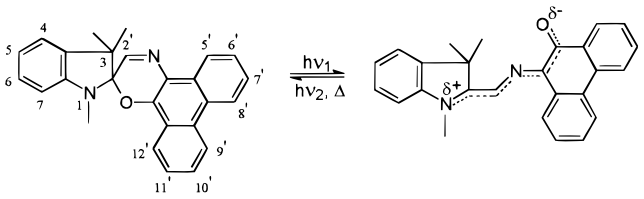

Ring-closed or spiro form of spirooxazine (SP)

Ring-open or merocyanine form of spirooxazine (MC)

pounds,[9,10] a property which may be advantageous in practical applications. However, our understanding of their photoisomerization dynamics is relatively limited.

The ultraviolet light-induced photochromism of SO is due to formation of extended π-conjugation following cleavage of their C(spiro)−O bonds (Scheme 1), which generates an intense absorption in the visible region.

The merocyanine (MC) form has a quinoidal nature characterized by a solvent sensitive absorption spectrum that red shifts as the medium polarity increases.[11] Photochemical transformations of SO molecules occur on subpicosecond time scales.[12−15] The MC form is generally less stable than the SP form and undergoes thermal ring-closing with a reaction half-time of $1-10^3$ s and an apparent activation energy of 14−30 kcal/mol.[9] This reaction can be accelerated by photoexcitation into the MC visible absorption band. Factors which stabilize the extended charge-delocalized state, e.g., electron donation into the MC indoline moiety, electron withdrawal from the MC oxazine moiety, and increasing solvent polarity, are expected to decrease the ring-closing rate constant.

We present herein results of kinetic studies of the dark reactions of several substituted spirooxazines following photoexcitation to their MC forms. These include observation of an apparent translocation of the dye from a polar internal site within the bilayer membrane to the aqueous−organic interface following ring-opening and a dramatic destabilization of the MC form upon coordination to a $Ru(bpy)_2^{2+}$ group, which manifests itself in both a shift in the thermal equilibrium position toward the SP form and a large increase in the thermal rate constant for ring-closing.

Experimental Section

Synthesis of SO. Compounds SO**1**−SO**3** and SO**7**−SO**9** (see Table 1 for structures) were prepared as described elsewhere[16] by coupling 9-amino-10-hydroxyphenanthrene hydrochloride (for SO**1**−SO**3**), 9-amino-10-hydroxy-2-nitrophenanthrene hydrochloride (for SO**7** and SO**9**), and 9-amino-10-hydroxy-4-nitrophenanthrene hydrochloride (for SO**8**) with substituted 2,3,3-trimethyl-3*H*-indolium iodides. Compounds SO**4**−SO**6** were prepared by coupling 6-hydroxy-5-nitroso-1,7-phenanthroline (for SO**4**) and 6-hydroxy-5-nitroso-1,10-phenanthroline (for SO**5** and SO**6**) with substituted 2,3,3-trimethyl-3*H*-indolium iodides. General synthetic procedures and product analyses including ^{1}H NMR spectral data are available as Supporting Information.

The $Ru(bpy)_2(SO)^{2+}$ complexes were prepared by following general protocols described in the literature.[17] Typically, 2.5 mg of $Ru(bpy)_2Cl_2$ and 2.0 mg of SO**5** or 3.2 mg of SO**6** were dissolved in 5 mL of a 9:1 ethanol/water mixture that had been deoxygenated by sparging with argon. The solutions were maintained under argon at 50 °C over the time course of the reaction, which was at least 69 h. Formation of $Ru(bpy)_2(SO5)^{2+}$ and $Ru(bpy)_2(SO6)^{2+}$ was monitored by following changes in the absorption spectra of the reaction solutions, as illustrated for $Ru(bpy)_2(SO6)^{2+}$ in Figure 1. Coordination was evident by the appearance of an intense absorption band at ∼420 nm, diagnostic of formation of $Ru(bpy)_2(phen)^{2+}$ complexes.[17] The syntheses were stopped

Table 1. Physical Properties of the Spirooxazines

Symbol	Compound	Solvent	λ_{max}^{SP} (nm)	λ_{max}^{MC} (nm)	k_f[a] (s^{-1})	k_1[b] (s^{-1})	k_{-1}[b] (s^{-1})
SO**1**	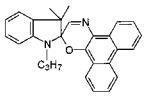	Methanol	342	602	4.1	0.07	4.1
		Pentane	344	568	0.16	0.006	0.16
		PC liposome	344	602	0.88	0.07	0.81
SO**2**	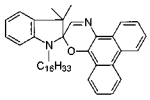	Methanol	342	602	1.8	0.04	1.8
		Pentane	344	570	0.14	0.002	0.14
		PC liposome	342	594	0.68	0.01	0.67
SO**3**	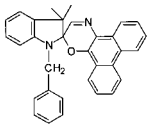	Methanol	344	596	10.6	0.07	10.5
		Pentane	342	564	0.12	0.006	0.12
		PC liposome	342	596	0.65	0.01	0.64
SO**4**	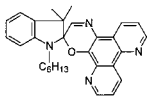	Methanol	354	602	0.39	0.02	0.37
		Pentane	344	568	0.34	0.001	0.34
		PC liposome	354	606	0.09	0.001	0.09
SO**5**	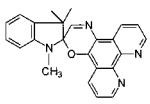	Methanol	344	590	0.31	0.01	0.3
		Pentane	340	564	0.28	0.0015	0.28
		PC liposome	346	594	0.43	0.03	0.40
SO**6**	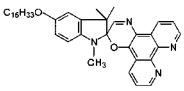	Methanol	350	608	0.15	0.02	0.13
		Pentane	342	584	0.25	0.01	0.25
		PC liposome	∼355	612	0.21	0.04	0.17
SO**7**	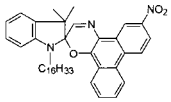	Methanol	∼340	602	0.30	0.01	0.29
		Pentane	≤ 400	584	0.18	0.002	0.18
		PC liposome	≤ 400	604	0.14	0.04	0.10
SO**8**	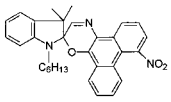	Methanol	342	598	0.58	0.02	0.56
		Pentane	346	576	0.15	0.0007	0.15
		PC liposome	350	600	0.38	0.03	0.35
SO**9**	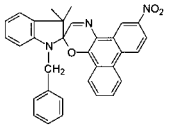	Methanol	≤ 400	598	3.4	0.2	3.2
		Pentane	≤ 400	576	0.13	0.001	0.13
		PC liposome	≤ 400	602	0.35	0.04	0.31
SO**10**	$Ru(bpy)_2(SO5)^{2+}$	Methanol	-	590	68		68
SO**11**	$Ru(bpy)_2(SO6)^{2+}$	Methanol	-	610	63		63

[a] At 23 °C. [b] Based upon an uncertainty of ∼50% in the merocyanine extinction coefficients,[11,21,22] the estimated accuracies of k_1 and k_{-1} are ±70% and ±5%, respectively.

(9) Chu, N. Y. C. In *Photochromism: Molecules and Systems*; Durr, H., Bouas-Laurent, T. H., Eds.; Elsevier: Amsterdam, 1990; pp 493−509.
(10) Baillet, G.; Giusti, G.; Guglielmetti, R. *J. Photochem. Photobiol. A: Chem.* **1993**, *70*, 157−161.
(11) Pozzo, J.-L.; Samat, A.; Guglielmetti, R.; De Keukeleire, D. *J. Chem. Soc., Perkin Trans. 2* **1993**, 1327−1332.
(12) Wilkinson, F.; Worral, D. R.; Hobley, J.; Jansen, L. Williams, S. L.; Langley, A. J.; Matousek, P. *J. Chem. Soc., Faraday Trans.* **1996**, *92*, 1331−1336.
(13) Zhang, J. Z.; Schwartz, B. J.; King, J. C. *J. Am. Chem. Soc.* **1992**, *114*, 10921−10927.
(14) Tamai, N.; Masuhara, H. *Chem. Phys. Lett.* **1992**, *191*, 189−194.
(15) Ernsting, N. P.; Arthen-Engeland, T. *J. Phys. Chem.* **1991**, *95*, 5502−5509.
(16) (a) Metelitsa, A. V.; Knyazhansky, M. I.; Palchkov, V. A.; Zubkov, O. A.; Vdovenko, A.V.; Shelepin, N. E.; Minkin, V. I. *Mol. Cryst. Liq. Cryst.* **1994**, *246*, 33−36. (b) Paltchkov, V. A.; Shelepin, N. E.; Minkin, V. I.; Trofimova, N. S.; Zoubkov, O. A. PCT Int. Appl. WO96/03368 (C1. CO7D 498110), 8 Feb 1996, Fr. Appl. 94/00918, 22 Jul 1996; 34 pp.
(17) Crosby, G. A.; Elfring, W. H. *J. Phys. Chem.* **1976**, *80*, 2206−2211.

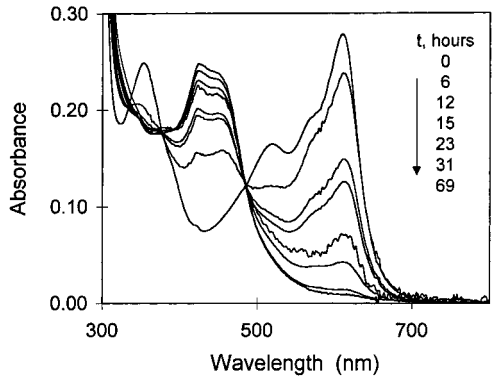

Figure 1. Changes in absorption spectra accompanying reaction of 10^{-3} M $Ru(bpy)_2Cl_2$ with 10^{-3} M SO**6** in 5 mL of methanol, recorded at 1:41 dilution.

10 h after the point that no further changes occurred in the solution absorption spectra. Coordination caused the characteristic absorption of the ring-opened MC form of the dyes at ~610 nm to disappear (Figure 1). The compounds decomposed upon adsorption to C25 Carboxymethyl Sephadex cation-exchange resin and so were not further purified.

Liposome Preparation. Phosphatidylcholine (PC) was extracted from fresh hen egg yolk and purified using chromatographic procedures described in the literature.[18] SO-containing unilamellar liposomes with average radii of 50 nm were prepared by high-pressure extrusion[19] using the explicit procedures described in the Supporting Information. SO/PC molar ratios were adjusted so that the average number of SO molecules in each liposome was between 5 and 50.

Optical Measurements. Continuous photolysis experiments were performed using a 1.5-kW xenon lamp whose output was focused and passed through aqueous $CuSO_4$ and UG11 (light transmission between 260 and 390 nm) or OG590 (light transmission at $\lambda > 560$ nm) Schott glass filters. The filtered light was then passed via an optical fiber bundle to the reaction cuvette that was mounted in a Hewlett-Packard 8452 diode array spectrophotometer interfaced to a ChemStation data acquisition/analysis system. Light intensities were measured with a calibrated PowerMax 500D laser power meter thermostated at room temperature; with the UG11 filter in place, the values obtained were 5×10^{-9}–5×10^{-8} einstein/(cm^2·s).

Absorption spectra and decay kinetics of photoinduced intermediates were measured by laser flash photolysis using a transient spectrophotometer whose general characteristics have been described.[20] The third harmonic (355 nm) from a Continuum Surelite III Nd:YAG laser was used as the excitation source; optical absorbances of samples were maintained below 0.1. Fluorescence measurements were made using a PTI model A1010 fluorescence spectrometer.

Results and Discussion

General Photochromic Behavior. Ultraviolet illumination of SO solutions caused the absorption intensity in the visible region to increase, whereas illumination into the visible band caused it to photobleach. For all compounds, the optical spectrum obtained upon thermal equilibration following UV photoexcitation was the same as that observed before illumination, indicating that the photoisomerization reactions were reversible. The nature of the optical changes that occur is illustrated in Figure 2, where the absorption spectra of SO**5** in methanol maintained in the dark and under continuous UV illumination are compared. The time dependence of absorbance changes at 590 nm (the peak maximum for MC**5**, the merocyanine form of SO**5**) under alternating cycles of UV light and dark is shown in Figure 3. The solid lines in Figure 3 correspond to exponential fits of the MC**5** thermal equilibration with an apparent rate constant $k_f = 0.28 \pm 0.01$ s^{-1}; this constant was independent of the spirooxazine concentration over the range 5×10^{-6}–2×10^{-5} M and the intensity of the UV light over the range 5×10^{-9}–5×10^{-8} einstein/(cm^2·s). Note that $k_f = k_1 + k_{-1}$, where k_1 and k_{-1} are the respective thermal rate constants for the ring-opening and ring-closing steps, i.e.:

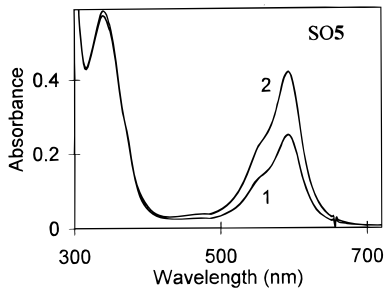

Figure 2. Absorption spectra of 1.1×10^{-5} M SO**5** in methanol (1) in the dark and (2) under steady-state ultraviolet illumination using UG11-filtered light (5×10^{-8} einstein/(cm^2·s)).

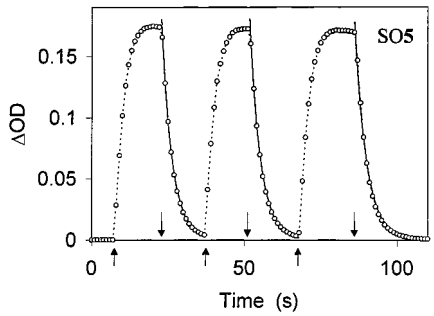

Figure 3. Absorbance changes at 590 nm of 1.1×10^{-5} M SO**5** in methanol following periodic ultraviolet illumination using UG11-filtered light (5×10^{-8} einstein/(cm^2·s)). Upward and downward arrows show intervals where the sample was exposed to or protected from the light. The solid lines correspond to exponential fits of the absorbance decay using a first-order rate constant $k_f = 0.28$ s^{-1}.

$$\mathrm{SP} \underset{k_{-1}}{\overset{k_1}{\rightleftharpoons}} \mathrm{MC} \qquad (1)$$

For SO**1**–SO**3**, SO**7**, $Ru(bpy)_2(SO5)^{2+}$ and $Ru(bpy)_2(SO6)^{2+}$, only very small changes were observed in the visible absorption upon continuous illumination, suggesting that thermal equilibration rates for these compounds were fast. In these cases, laser flash photolysis was used to obtain transient absorption spectra and the kinetics of thermal reequilibration. As an example, transient absorption spectra of $Ru(bpy)_2(SO5)^{2+}$ are shown in Figure 4 at three different times following the laser pulse. The solid line in Figure 4 gives the absorption spectrum in methanol of MC**5**. The near-coincidence of the transient absorption spectra with the spectrum of MC**5** indicates that excitation of $Ru(bpy)_2(SO5)^{2+}$ at 355 nm causes ring-opening on the SO**5** ligand. Complete recovery of the $Ru(bpy)_2(SO5)^{2+}$ absorption spectrum was observed in the dark. The kinetic waveform for transient absorption decay at 610 nm is reproduced in Figure 5; the smooth curve is the theoretical fit for exponential decay with a rate constant $k_f = 68$ s^{-1}. The rate constants for thermal equilibration of all compounds measured in different solvents ranged from 10^{-1} to 10^2 s. Representative data obtained in methanol, pentane, and PC liposomal suspensions are summarized in Table 1.

(18) Singleton, W. S.; Gray. M. S.; Brown, M. L.; White, J. L. *J. Am. Oil Chem. Soc*. **1965**, *42*, 53–56.
(19) Mayer, L. D.; Hope, M. J.; Cullis, P. R. *Biochim. Biophys. Acta* **1986**, *858*, 161–168.
(20) Lymar, S. V.; Khairutdinov, R. F.; Soldatenkova, V. A.; Hurst, J. K. *J. Phys. Chem*. **1998**, *102*, 2811–2819.

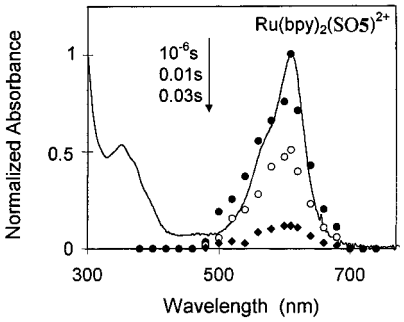

Figure 4. Transient absorption spectra of 2×10^{-5} M Ru(bpy)$_2$(SO**5**)$^{2+}$ in methanol at different times following 355-nm laser flash excitation (points) and the visible absorption spectrum of 2×10^{-5} M SO**5** in methanol (solid line).

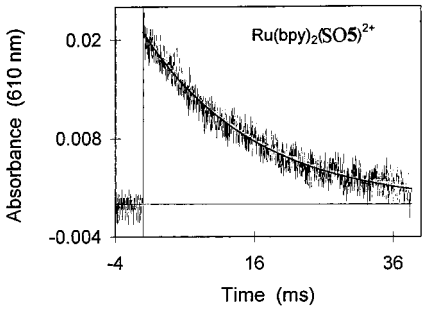

Figure 5. Decay kinetics of the 355-nm laser pulse-induced transient absorption at 610 nm for 2×10^{-5} M Ru(bpy)$_2$(SO**5**)$^{2+}$ in methanol and the exponential fit with a rate constant $k = 68$ s^{-1} (solid line).

For SO**6**, the relative amounts of SP and MC in methanol and chloroform were determined at room temperature by NMR spectroscopy.[11] From these data, the isomer equilibrium constants (K = [MC]/[SP]) were calculated to be K(MeOH) = 0.38 and K(CHCl$_3$) = 0.23. Using these values, the corresponding molar extinction coefficients for the MC visible band maxima (ϵ_λ) were calculated to be ϵ_{608}(MeOH) = 1.2×10^5 M^{-1} cm^{-1} and ϵ_{612}(CHCl$_3$) = 9.3×10^4 M^{-1} cm^{-1}. In general, MC ϵ_λ values are relatively insensitive to both the nature of substituent groups on the indoline and oxazine rings and solvent polarities.[11,21,22] Consequently, we have used the average value for the SO**6** extinction coefficient, i.e., $\epsilon_\lambda \approx 1 \times 10^5$ M^{-1} cm^{-1}, to estimate the isomer equilibrium constants for the other SO. Values for the ring-opening (k_1) and ring-closing (k_{-1}) rate constants were then evaluated using the relationships $K = k_1/k_{-1}$ and $k_f = k_1 + k_{-1}$. Results obtained for reactions in methanol, pentane, and PC liposomes are summarized in Table 1 and Figure 6.

Substituent Effects upon the Reaction Dynamics. Substituents on the spirooxazine rings can influence the rates of ring-opening and -closing through both electronic and steric effects. Steric repulsion favoring formation of the SP form has been documented for the structurally similar spiropyrans when substituted at the 3-position of the pyran ring and/or alkylated at the heterocyclic nitrogen atom.[23] Electronic effects are usually interpreted in terms of their influence upon the extent of charge separation in the MC form; i.e., substituents that increase the electronic charge on the indoline N and oxazine O atoms (Scheme 1) destabilize the MC form, and vice versa.

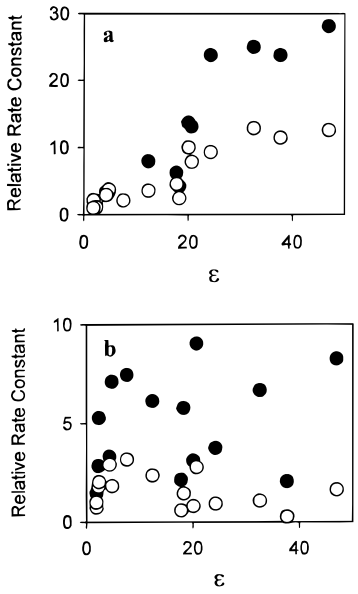

Figure 6. Dependence of k_1 (closed circles) and k_{-1} (open circles) for SO**2** (panel a) and SO**5** (panel b) upon the solvent dielectric constant (ϵ). The values of the rate constants relative to the rate constants in pentane are shown. The solvents used (with ϵ in parentheses)[39] were pentane (1.84), hexane (1.89), benzene (2.28), toluene (2.38), diethyl ether (4.33), $CHCl_3$ (4.8), tetrahydrofuran (7.6), pyridine (12.4), 1-butanol (17.8), 2-propanol (18.3), 1-propanol (20.1), ethanol (24.3), methanol (32.6), glycol (37.7), glycerol (42.5), and dimethyl sulfoxide (46.7).

For the compounds investigated here, consideration of the substituent ring positions suggests that steric effects will be relatively minor. Apart from the large increase in k_{-1} accompanying Ru(bpy)$_2^{2+}$ coordination of the *o*-phenanthroline moieties (Figure 2), ring-closing rate constants were relatively insensitive to substitution, and systematic trends were observed only in polar solvents and PC liposomes. In these environments, addition of nitro substituents caused k_{-1} to decrease 2−8-fold (compare SO**7**−SO**9** with SO**1**−SO**3**). This effect is of the same magnitude as that observed for the thermal equilibration rate constant of spiropyrans bearing small electron-withdrawing substituents[24] and can be rationalized in terms of charge reduction on the oxazine O atom, thereby lowering attractive electrostatic interactions with the indoline cation and raising the activation energy for ring-closing. Replacement of N-alkyl substituents with a benzyl group caused 2−10-fold increases in k_{-1} (compare SO**3** with SO**1**, SO**2**, and SO**9** with SO**7**) This rate acceleration can be similarly understood in terms of inductive withdrawal of electron density from the N atom, increasing its susceptibility to nucleophilic attack by the oxazine O atom (Scheme 1). One should note, however, that the absence of similar substituent effects in nonpolar media suggests that this simple analysis is naïve.

The unusually large rate enhancement in k_{-1} accompanying Ru(bpy)$_2^{2+}$ coordination to SO**5** and SO**6** through their modified oxazine rings is probably also electronic in origin. Among the transition metals, ruthenium(II) has the greatest propensity for π-back-bonding of d electron density into symmetry-matched unoccupied ligand orbitals.[25] In this case, electron donation into the delocalized *o*-phenanthroline π*-orbitals should significantly increase the negative charge on the oxazine O atom, facilitating

(21) Wilkinson, F.; Hobley, J.; Naftaly, M. *J. Chem. Soc., Faraday Trans.* **1992**, *88*, 1511−1517.
(22) Hobley, J.; Wilkinson, F. *J. Chem. Soc., Faraday Trans.* **1996**, *92*, 1323−1330.
(23) Guglielmetti, R. In *Photochromism: Molecules and Systems*; Durr, H., Bouas-Laurent, T. H., Eds.; Elsevier: Amsterdam, 1990; pp 314−466.
(24) Bertelson, R. C. In *Photochromism*; Brown, G. H., Ed.; Wiley-Interscience: New York, 1971; pp 45−432.
(25) (a) Taube, H. *Adv. Chem. Ser.* **1997**, *253*, 1−17. (b) Taube, H. *Survey Prog. Chem.* **1973**, *6*, 1−46.

both the ring-closing rate (Figure 2) and stabilization of the SP isomer (Figure 1).

Solvent Effects upon the Reaction Dynamics. Reactions that involve increasing charge separation in the transition state generally proceed more rapidly in polar solvents, and vice versa. Correlations of this nature have formed the basis for free energy relationships[26] defining the "ionizing power" of solvents, i.e., their ability to stabilize the developing charge. For the compounds containing phenanthrene units (SO**1**−SO**3**, SO**7**−SO**9**), the expected correlation was observed for the ring-opening rate constants, which increased progressively with increasing dielectric constant of the solvent (Table 1, Figure 6a). However, the reverse ring-closing reactions also gave progressively larger k_{-1} values with increasing solvent polarity (Table 1, Figure 6a), contrary to expectations based upon a simple charge separation model. Furthermore, no systematic solvent dependence was observed in either k_1 or k_{-1} values for the corresponding phenanthroline-based compounds (SO**4**−SO**6**, Figure 6b). Since there were no significant differences between reaction rates in protic and polar aprotic solvents with the same polarities (Figure 6), specific solvation effects are probably not important. The results therefore suggest that, for the phenanthrene-based compounds, the transition state is more polar than either the SP or MC forms. This circumstance could arise if, in approaching the transition state, there is loss of pseudo π-conjugation between the indoline and oxazine units, increasing the electronic charge on the N and O atoms and, thereby, the molecular dipole moment. π-Conjugation implies that the indoline and oxazine rings are approximately coplanar. The reaction coordinate for formation of the SP spiro ring would therefore quite naturally involve torsional twisting of these units with attendant charge localization on N and O. This model is consistent with recent ab initio calculations indicating that ring-opening reactions of pyrans and related compounds follow a two-step mechanism involving primarily C−O bond cleavage followed by rotation about the C−C single bond.[27] The absence of a demonstrable solvent dependence for k_{-1} for the phenanthroline-based analogues implies that, for these compounds, the MC and transition-state polarities are comparable; the independence of k_1 upon solvent remains problematical, however. Guglielmetti and coworkers have also reported that the thermal fading rate constants (k_f) for these compounds are insensitive to solvent polarity.[11] Ultimately, determining the origin of these solvent effects will require additional study.

Solvent Effect on the SO Absorption Spectra. The absorption maxima of MC forms of the dyes produced by steady-state UV illumination of SO solutions coincided with absorption maximum of the ring-opened forms of SO molecules measured before illumination (Figure 2). In all cases, decreasing the solvent polarity caused the visible absorption maxima of the MC forms of the dyes to shift by ∼20−30 nm to shorter wavelengths but had little effect on the position of the UV absorption maxima (Table 1). In Figure 7, the wavelength of the band maximum for SO**5** is plotted against the solvent dielectric constant (ϵ). The dependence of λ_{max} on ϵ is approximated by the solid line given by the equation.

$$\lambda_{max} = a_1 + \frac{a_2\epsilon}{1+\epsilon} \qquad (2)$$

The best fit to the experimental data was obtained with a_1 = 531 nm and a_2 = 66 nm.[28] The hypsochromic shift of the absorption maximum for the ring-opened form with decreasing solvent polarity is typical of spirooxazines[11] and may be explained by invoking a higher polarity in the MC excited state than in the ground state arising from indoline-to-oxazine transfer of electron density. Consequently, as solvent polarity decreases, the excited state is destabilized relative to the ground state, and the absorption band is blue-shifted.

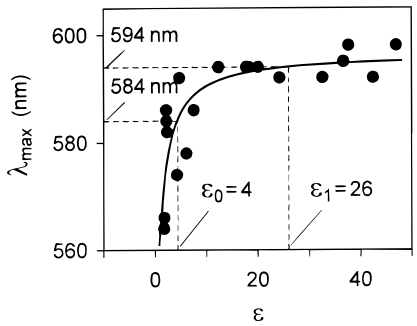

Figure 7. Dependence of λ_{max} for MC**5** upon the solvent dielectric constant (ϵ). The solvents used (with ϵ in parentheses)[39] were pentane (1.84), hexane (1.89), dioxane (2.21), benzene (2.28), toluene (2.38), diethyl ether (4.33), $CHCl_3$ (4.8), acetic acid (6.15), tetrahydrofuran (7.6), pyridine (12.4), 1-butanol (17.8), 2-propanol (18.3), 1-propanol (20.1), ethanol (24.3), methanol (32.6), dimethylformamide (36.7), glycol (37.7), glycerol (42.5), and dimethyl sulfoxide (46.7). The solid line shows the best fit of experimental data by eq 2. Dashed horizontal lines correspond to λ_{max} of the merocyanine form of SO5 at $t = 10^{-6}$ s after the laser pulse (584 nm) and after 5 s of continuous UV illumination of the same solution (594 nm).

Table 2. Properties of the PC Liposomal Microenvironment for the MC Forms

compound	ϵ_0[a]	ϵ_1[b]	r_0 (nm)[c]	r_1 (nm)[c]	τ (ms)[d]
SO**1**	30	30	1.9	1.9	
SO**2**	9	9	1.7	1.7	
SO**3**	25	25	1.9	1.9	
SO**4**	5	40	1.6	2.0	1.9
SO**5**	4	26	1.5	1.9	1.6
SO**6**	5	36	1.6	2.0	2.3
SO**7**	14	14	1.7	1.7	
SO**8**	28	28	1.9	1.9	
SO**9**	35	35	2.0	2.0	

[a] Apparent dielectric constant immediately following photoexcitation. [b] Apparent dielectric constant in the photostationary state. [c] Estimated distance from the bilayer center. [d] Characteristic time for movement from site 0 to site 1.

The wavelengths of the MC visible band maxima obtained in PC liposomes are similar to the wavelengths measured in polar solvents, indicating that the ring-opened forms are located in a relatively polar microenvironment within the membrane. We have used these solvatochromic properties to estimate dielectric constant of the MC microenvironment within the membrane. As an example, the upper horizontal dashed line in Figure 7 corresponds to the absorption maximum (λ_{max} = 594 nm) of the ring-opened form of SO**5** in the liposome. Extrapolation from its point of intersection with the solid line to the abscissa suggests an effective dielectric constant for MC**5** of $\epsilon \approx 26$. Apparent dielectric constants estimated for the other liposome-bound MC are listed in Table 2.

Intramembrane Diffusion of MC. Immediately after the laser pulse, the absorption spectra of MC**4**−MC**6** in PC liposomes were blue-shifted relative to their spectra at longer

(26) Reichardt, C. *Angew. Chem., Intl. Ed. Engl.* **1965**, *4*, 29−40.
(27) Day, P. N.; Wang, Z.; Pachter, R. *J. Phys. Chem.* **1995**, *99*, 9730−9738.
(28) Equation 2 is empirical and was used solely because it approximates well the experimental data. No particular physical meaning is attached to its form.

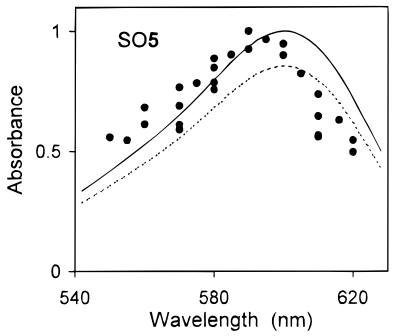

Figure 8. Normalized transient absorption spectrum of a 2 mM PC liposome suspension in 0.01 M potassium phosphate buffer, pH 8.0, containing 5×10^{-6} M SO**5** at 10^{-6} s after laser flash excitation at 355 nm (points) and the normalized absorption spectrum after 5 s of continuous UV illumination of the same solution (solid line). The dashed line shows the absorption spectrum obtained from continuous illumination scaled to intersect the transient absorption spectrum at the isosbestic wavelength ($\lambda = 604$ nm).

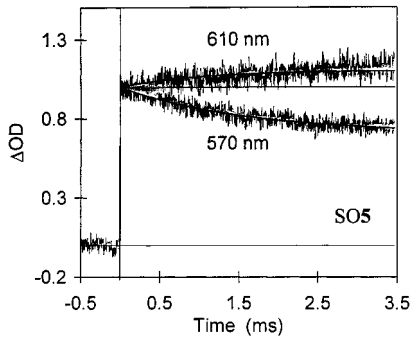

Figure 9. Decay kinetics at 610 and 570 nm of the laser pulse-induced transient absorption changes of a 2 mM PC liposome suspension in 0.01 M potassium phosphate buffer, pH 8.0, containing 5×10^{-6} M SO**5** and the exponential best fits (solid lines) of the experimental data using eqs 3 and 4.

observation times, but they were subsequently red-shifted to their equilibrium positions within milliseconds following the laser pulse. As an example, the transient absorption spectrum for MC**5** at 10^{-6} s after laser flash excitation is given in Figure 8 (points). Comparison to the normalized absorption spectrum obtained upon continuous illumination of the same suspension (solid line) shows that the spectrum of the initially formed transient was blue-shifted by ~10 nm. This shift was manifested in absorbance increases at wavelengths shorter than the wavelength of the MC final absorption maximum and decreases at wavelengths longer than the maximum (Figure 9). No transient absorption changes were observed at 604 nm, indicating that this wavelength is isobestic for the two absorbing forms.

No transient changes in the MC absorption spectrum were observed for liposome-bound spirooxazines possessing phenanthrene moieties (SO**1**−SO**3**, SO**7**−SO**9**) in place of phenanthrolines. Further, no transient changes in the MC absorption spectrum were observed for any SO in methanol or pentane. In these cases, the MC transient spectra obtained at 10^{-6} s by laser flash photolysis coincided with the spectra obtained by continuous illumination.

The red shift in the transient peak maxima of SO**4**−SO**6** in liposomes might arise from movement of the initially formed MC from the less polar hydrocarbon interior to a more polar site in the interfacial region of the membrane. The values of the apparent dielectric constant of the membrane microenvironment around the initially formed MC**4**−MC**6** were estimated from the dependence of the band maxima upon the solvent dielectric constant as before. For example, the lower horizontal dashed line in Figure 7 corresponds to the absorption maximum ($\lambda_{max} = 584$ nm) of MC**5** at 10^{-6} s after the laser pulse. Its intersection points with the solid line correspond to a dielectric constant of $\epsilon \approx 4$.

A potential alternative explanation for the observed spectral shifts is that the SO molecules are aggregated within the PC liposome membrane and undergo slow disaggregation following rapid photoinitiated cleavage of their C(spiro)−O bond. The tendency for spiropyrans[29] and other dyes[30] to undergo aggregation in organic membranes and films is well-known. Three types of dye aggregates have been defined—dimers, H-aggregates, and J-aggregates.[31] The spectra of dimers and H-aggregates are blue-shifted relative to the molecularly dispersed monomers, whereas J-aggregates are red-shifted. Consequently, the blue-shifted absorption spectra of MC**4**−MC**6** observed immediately after the laser pulse can be explained by aggregation only if they exist at short times in the form of dimers and/or H-aggregates or if MC J-aggregates are formed following photoisomerization of monomeric or H-aggregated SP forms. The J-aggregates generally possess intense fluorescence bands that are red-shifted relative to their corresponding monomers, whereas the fluorescence quantum yields of H-aggregates and dimers are very low compared to those of the monomers.

For SO**1**−SO**6**, a nearly structureless fluorescence was detected in the wavelength range 400−500 nm with λ_{max} at ~450 nm. The emission quantum yields were O_2-independent, identical in PC liposomes and when molecularly dispersed in methanol or pentane, and independent of the SO/liposome molar ratio over a range corresponding to 5−50 SO molecules per liposome. The emission spectral band shapes were also independent of SO concentrations. Fluorescence intensities of the NO_2-substituted spirooxazines SO**7**−SO**9** were very weak. These observations therefore give no evidence for aggregation of the dyes in the membrane, supporting the alternative interpretation that the spectral shifts are induced by changes in medium polarity and represent relocation within the membrane following photoisomerization of the SP form of SO**4**−SO**6** molecules to the corresponding MC forms.

The dependence of ϵ upon distance from the membrane bilayer center is depicted in Figure 10, which is an adaptation from recent calculations[32] based upon X-ray and neutron diffraction studies on dioleoylphosphatidylcholine bilayer membranes[33] using a model for the interface consisting of a gradual two-step transition between three phases.[34] The horizontal dashed lines in Figure 10 correspond to the values of the dielectric constant of the medium around MC**5** at $t = 10^{-6}$ s after the laser pulse ($\epsilon_0 = 4$) and during continuous UV illumination of the same solution ($\epsilon_1 = 26$). From their points of intersection with the solid line, we estimate that following photoinitiated ring-opening, the MC diffuses ~0.4 nm from a position $r_o \approx 1.5$ nm from the bilayer center to $r_1 \approx 1.9$ nm from the center. This corresponds roughly to movement from the region containing the acyl carbonyl groups of the glycerol backbone to the interfacial region containing the phosphate

(29) Seki, T.; Ichimura, K. *J. Phys. Chem.* **1990**, *94*, 3769−3775.
(30) See, e.g.: Song, X.; Perlstein, J.; Whitten, D. G. *J. Am. Chem. Soc.* **1997**, *119*, 9144−9159 and references therein.
(31) Kasha, M.; Rawls, H. R.; El-Bayoumi, M. A. *Pure Appl. Chem.* **1965**, *11*, 371−392.
(32) Mazeres, S.; Schram, V.; Tocanne, J.; Lopez, A. *Biophys. J.* **1996**, *71*, 327−335.
(33) Wiener, M. C.; White, S. H. *Biophys. J.* **1992**, *61*, 434−447.
(34) Sanders, C. R., II; Schwonek, J. P. *Biophys. J.* **1993**, *65*, 1207−1218.

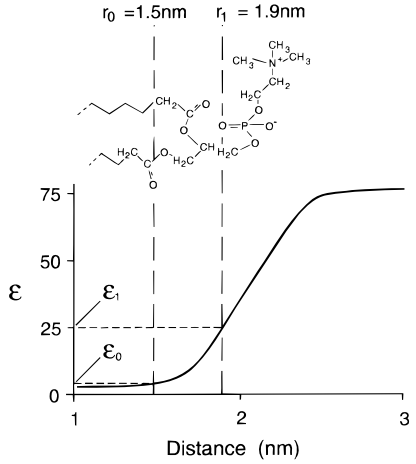

Figure 10. Variation in bilayer membrane dielectric constant (ϵ) with distance from the membrane center (adapted from ref 32). The positions of MC**5** immediately after laser pulse excitation and in steady state, deduced from the corresponding visible band maxima, are indicated by r_o and r_1, respectively.

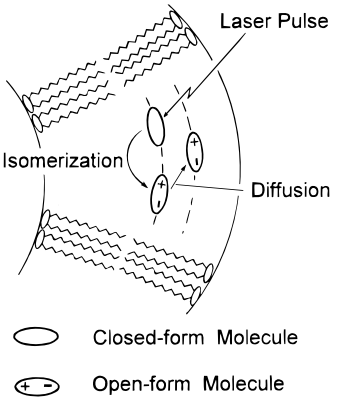

Figure 11. Schematic drawing of the processes following laser pulse excitation of phenanthroline-containing spirooxazine molecules within the PC liposomal membrane.

headgroups. This relocation is illustrated stylistically in Figure 11. Values of r_o and r_1 for the other MC are summarized in Table 2.

Diffusion Dynamics. Kinetic analyses were made on the transient decay profiles to determine the characteristic times for movement of MC**4**−MC**6** within the PC membrane. The normalized kinetic waveforms of transient absorption changes for MC**5** (Figure 9) were analyzed quantitatively by using the following equations, which describe exponential decay:

$$\Delta OD_{570} = a_1 + (1 - a_1)\exp(-t/\tau) \quad (3)$$

$$\Delta OD_{610} = 1 + a_2(1 - \exp(-t/\tau)) \quad (4)$$

In eqs 3 and 4, $(1 - a_1)$ and a_2 are constants representing the total amplitudinal changes at 570 and 610 nm, respectively, and τ is the characteristic time of the movement of the MC**5** from the initial to final intermembrane site. The best-fit values for τ to the experimental data (shown in Figure 9 as solid lines) were obtained with $\tau = 1.6 \times 10^{-3}$ s. Comparable values were obtained for MC**4** and MC**6** (Table 2).

The characteristic times measured for MC**4**−MC**6** relocation ($\tau \approx 10^{-3}$ s) are much greater than diffusion times usually observed for neutral molecules in PC liposomal membranes ($\tau_D \leq 10^{-7}$ s),[35−38] indicating the existence of energetic traps for SP**4**−SP**6** at ∼1.5 nm from the membrane center. The depth of the trap (E_T), evaluated from the equation $\tau^{-1} \sim 10^{12} \exp(-E_T/RT)$, is ∼50 kJ/mol. This region also contains some H_2O,[33] so it is possible that the traps originate in water-mediated H-bonding interactions between the heterocyclic N atoms of the phenanthroline rings and the O atoms of the phospholipid acyl ester carbonyl moieties.

The absence of detectable transient changes in the MC absorption spectra for phenanthrene-containing SO**1**−SO**3** and SO**7**−SO**9** in PC liposomes might be due either to more rapid relocation, with $\tau < 10^{-6}$ s, indicative of shallower traps for the SP forms of these compounds, or to initial placement of the SP form in more polar locations within the membrane. Since λ_{max} is insensitive to solvent polarity when $\epsilon > 20$ (Figure 7), changes in transient absorption will be very small if these SP are located in more polar regions of the membrane than SP**4**−SP**6**. In any event, the behavioral differences noted appear to be attributable to specific interactions of the phenanthroline N atoms with components of the liposome.

Acknowledgment. Funding for the research at Washington State University was provided by the Division of Chemical Sciences, Office of Basic Energy Sciences, U.S. Department of Energy, under Grant DE-FG06-95ER14581 (to J.K.H.). Funding for the research at Rostov University was provided by the U.S. Civilian Research and Development Foundation for the Independent States of the Former Soviet Union (CRDF) under Grant RCI-250 (to V.I.M.).

Supporting Information Available: General synthetic protocols, melting points, elemental analyses, and 300-MHz ^{1}H NMR spectral data for compounds SO**1**−SO**9**; procedures for preparation of SO-doped liposomes (5 pages, print/PDF). See any current masthead page for ordering information and Web access instructions.

JA9825985

(35) Evaluated from the Einstein−Smoluchowskii equation: $\tau_D \approx l^2/D$, where l is the average distance of the movement and D is the diffusion coefficient. In the calculation of τ_D, we used $l = 0.4$ nm and $D \geq 10^{-8}$ cm^2 s^{-1}.

(36) Alper, H. E.; Stouch, T. R. *J. Phys. Chem.* **1995**, *99*, 5724−5731.
(37) Mason, R. P.; Chester D. W. *Biophys. J.* **1989**, *56*, 1193−1201.
(38) Vaz, W. L. C.; Clegg, R. M.; Halman, D. *Biochemistry* **1985**, *24*, 781−786.
(39) Handbook of Chemistry and Physics, 71st ed.; Lide, D. R., Ed.; CRC Press: Boca Raton, FL, 1990; 9-10−9-11.